Theoretical & Applied Mechanics Letters 7 (2017) 117–120

Contents lists available at ScienceDirect

Theoretical & Applied Mechanics Letters

journal homepage: www.elsevier.com/locate/taml

Letter

Modeling on monitoring the growth and rupture assessment of saccular aneurysms

Yangkun Du [a], Chaofeng Lü [a,b,c,*]

[a] Department of Civil Engineering, Zhejiang University, Hangzhou 310058, China
[b] Key Laboratory of Soft Machines and Smart Devices of Zhejiang Province, Zhejiang University, Hangzhou 310027, China
[c] Soft Matter Research Center, Zhejiang University, Hangzhou 310027, China

HIGHLIGHTS

- A new strategy of using dielectric elastomer sensors to monitor the growth of saccular aneurysms.
- The correlation between the output capacitance and the growth state of the saccular aneurysm is established.
- A method of multiple indicator (size and wall stress) is demonstrated more reliable for evaluating the rupture risk of saccular aneurysms.

ARTICLE INFO

Article history:
Received 26 December 2016
Received in revised form
23 January 2017
Accepted 23 January 2017
Available online 27 February 2017
*This article belongs to the Solid Mechanics

Keywords:
Saccular aneurysms
Rupture risk
Dielectric elastomer capacitance sensor
Elastic growth theory
Finite deformation

ABSTRACT

The unpredictable rupture of saccular aneurysms especially of the intracerebral aneurysm is a knotty problem that always results in high mortality. Traditional diagnosis of medical images, which gives the aneurysm size and compares with a speculated critical size from clinical statistics, was demonstrated inadequate to forecasting rupture. Here, we propose a new detecting strategy that uses a dielectric elastomer (DE) capacitance sensor to monitor the growth of saccular aneurysms and deliver both the wall stress and geometric parameters. Based on the elastic growth theory together with the finite deformation analyses, the correlation between the real-time output capacitance of the DE sensor and the wall stress and/or geometry of an aneurysm is derived. Compared to clinic statistics and biomechanics simulations, the wall stress and geometric size may be used as combined indicators to assess the rupture risk of a saccular aneurysm. Numerical results show that an output relative capacitance of 30 indicates a high risk of rupture. Finally, the sensitivity and resolution of the DE sensor are proved adequately high for monitoring the growth state and evaluating the rupture risk of a saccular aneurysm.

© 2017 The Author(s). Published by Elsevier Ltd on behalf of The Chinese Society of Theoretical and Applied Mechanics. This is an open access article under the CC BY-NC-ND license (http://creativecommons.org/licenses/by-nc-nd/4.0/).

Saccular aneurysms are abnormal asymmetric dilation most commonly in the apex of cerebral bifurcations. Ruptured intracranial aneurysms always result in spontaneous subarachnoid hemorrhage (SAH) which has the mortality rate of about 35%–50% [1–3]. In clinic, there are two main methods to treat this aneurysm, one the intracranial surgery that uses a metal clip or metallic coils to isolate the aneurysm from the blood flow, the other the conservative management assuming that the aneurysm will not rupture [3–5]. Both methods need to evaluate the rupture risk of an aneurysm to determine the most suitable timing and method. The combination of lesion location, shape, and the blood pressure was recommended as the best indicators for rupture. In addition, according to the clinical statistics, the critical maximum dimension was suggested as 10 mm [3,4,6].

On the other hand, biomechanics simulations demonstrated that the wall shear stress (WSS) and the flow impingement play important roles in the rupture of saccular aneurysms. Shojima et al. [7] argued that a WSS of about 1.5 N/m^2 due to blood flow will induce the degeneration of endothelial cells in the aneurysm wall, and, therefore, the formation of lesion which further causes ruptures. In comparison, anatomical evidence shows that a typical human saccular aneurysm has a shape of perfect sphere (Fig. 1(a)) [8], and in terms of material strength, in vitro loading tests suggest 0.5 MPa as the critical Cauchy stress for rupture [9]. However, the in vivo wall stress of the aneurysm can neither be detected by the traditional clinical diagnosis methods nor addressed by the hemodynamics simulations.

Here, we propose to mount a dielectric elastomer (DE) capacitor sensor onto the outer surface of a saccular aneurysm so as to get its

* Corresponding author.
E-mail address: lucf@zju.edu.cn (C. Lü).

http://dx.doi.org/10.1016/j.taml.2017.01.007
2095-0349/© 2017 The Author(s). Published by Elsevier Ltd on behalf of The Chinese Society of Theoretical and Applied Mechanics. This is an open access article under the CC BY-NC-ND license (http://creativecommons.org/licenses/by-nc-nd/4.0/).

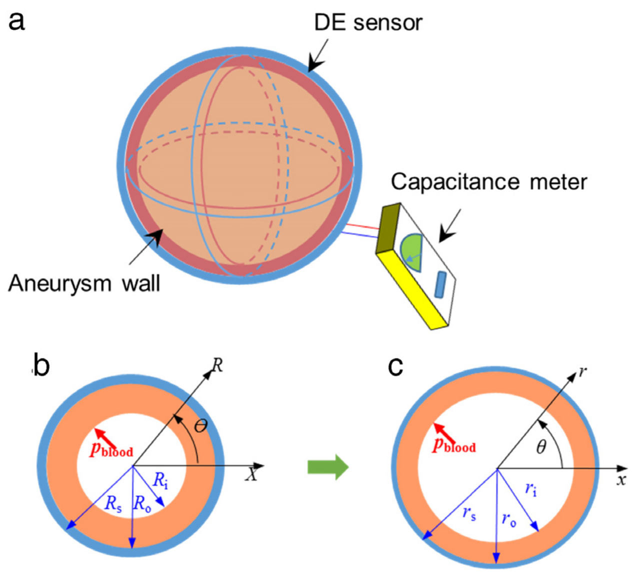

Fig. 1. (a) Theoretical modeling for monitoring the growth of a saccular aneurysm. (b) Cross section of the aneurysm along equatorial plane in reference configuration. (c) Cross section in current configuration.

real-time size and wall stress based on the output electric signals. In order to correlate the electric signals from the DE sensor to the geometrical and mechanical properties of the aneurysm, the elastic growth theory [10–14] is employed to account for the deformation due to both the natural growth and blood pressure. For simplicity of the modeling process, we assume that the saccular aneurysm is a perfect sphere (Fig. 1(b)) with uniform thickness [8] while the DE sensor contacts perfectly with the aneurysm without any slippage during deformation. Since the WSS ($\sim$1.5 N/m^2) created by the blood flow is far lower than the critical Cauchy stress (0.5 MPa) by an order of 10^6, the inner surface of the aneurysm wall is assumed shear traction free but under a constant blood pressure [15].

Figure 1 shows the simplified modeling, where R and r represent respectively the radii of the saccular aneurysm in the initial and current configuration, where the subscript "i" and "o" indicate the inner and outer surfaces of the aneurysm wall while "s" indicates the outer surface of the DE sensor. The overall deformation of the aneurysm is assumed in a spherical symmetry state, with a deformation gradient tensor of

$$\boldsymbol{F} = \operatorname{diag}\left(\lambda_r,\ \lambda_\theta,\ \lambda_\varphi\right) = \operatorname{diag}\left(\frac{\mathrm{d}r}{\mathrm{d}R},\ \frac{r}{R},\ \frac{r}{R}\right), \tag{1}$$

where λ is the principal stretch. The aneurysm is assumed to experience a diagonal anisotropic growth with the growth tensor $\boldsymbol{F}_\mathrm{g} = \operatorname{diag}\left(g_r,\ g_\theta,\ g_\varphi\right)$, where g is the growth factor. According to the decomposition principle suggested by Rodriguez et al. [13] that ensures the compatibility and/or integrity of the material body, the elastic deformation tensor is given by

$$\begin{aligned}\boldsymbol{F}_\mathrm{e} &= \boldsymbol{F}\cdot\boldsymbol{F}_\mathrm{g}^{-1} = \operatorname{diag}\left(\lambda_{\mathrm{e}r},\ \lambda_{\mathrm{e}\theta},\ \lambda_{\mathrm{e}\varphi}\right)\\ &= \operatorname{diag}\left(\frac{1}{g_r}\frac{\mathrm{d}r}{\mathrm{d}R},\ \frac{1}{g_\theta}\frac{r}{R},\ \frac{1}{g_\varphi}\frac{r}{R}\right).\end{aligned} \tag{2}$$

To find the stress field, we assume that the aneurysm wall follows the incompressible neo-Hookean law, for which the strain energy function is

$$W_\mathrm{A} = \frac{1}{2}\mu_\mathrm{A}\left(\lambda_{\mathrm{e}r}^2 + \lambda_{\mathrm{e}\theta}^2 + \lambda_{\mathrm{e}\varphi}^2 - 3\right) - p(\lambda_{\mathrm{e}r}\lambda_{\mathrm{e}\theta}\lambda_{\mathrm{e}\varphi} - 1), \tag{3}$$

where $\lambda_{\mathrm{e}r}\lambda_{\mathrm{e}\theta}\lambda_{\mathrm{e}\varphi} = 1$, μ_A is the initial shear modulus of the aneurysm, p is the hydrostatic pressure to be determined. In terms of principal stretches, the Cauchy stresses of the aneurysm are obtained as

$$\sigma_{rr}^{(\mathrm{A})} = \mu_\mathrm{A}\lambda_{\mathrm{e}r}^2 - p = \mu_\mathrm{A}\lambda_{\mathrm{e}\theta}^{-4} - p, \tag{4a}$$

$$\sigma_{\theta\theta}^{(\mathrm{A})} = \sigma_{\varphi\varphi}^{(\mathrm{A})} = \mu_\mathrm{A}\lambda_{\mathrm{e}\theta}^2 - p. \tag{4b}$$

For the incompressible condition, we can get from Eq. (2) the differential equation

$$\frac{r^2}{R^2}\frac{\mathrm{d}r}{\mathrm{d}R} = g_r g_\theta g_\varphi. \tag{5}$$

This forms the equation governing the deformation induced by the volumetric growth. The solution to Eq. (5) is

$$r^3 - r_\mathrm{i}^3 = g_r g_\theta g_\varphi\left(R^3 - R_\mathrm{i}^3\right), \quad R_\mathrm{i} \le R \le R_\mathrm{o}. \tag{6}$$

As for the DE sensor, no growth occurs and the elastic gradient tensor is $\boldsymbol{F}_\mathrm{e} = \operatorname{diag}\left(\lambda_r,\ \lambda_\theta,\ \lambda_\varphi\right) = \operatorname{diag}\left(\frac{\mathrm{d}r}{\mathrm{d}R},\ \frac{r}{R},\ \frac{r}{R}\right)$. The material of the DE sensor is assumed to satisfy the following amendatory incompressible neo-Hookean law [16],

$$\Omega_\mathrm{D} = \frac{1}{2}\mu_\mathrm{D}\left(\lambda_r^2 + \lambda_\theta^2 + \lambda_\varphi^2 - 3\right) + H\left(\lambda_r\lambda_\theta\lambda_\varphi - 1\right) + \varepsilon_0^{-1}\beta I_5, \tag{7}$$

where $\lambda_r\lambda_\theta\lambda_\varphi = 1$, μ_D, ε_0, and β are respectively the initial shear modulus of the DE sensor, the permittivity of the vacuum, and the relative electroelastic coupling parameter, H the hydrostatic pressure to be determined, and I_5 the invariant of the coupling tensor between the electric field and the mechanical field [16]. Since the permittivity of the DE material is of the order 10^{-11} and the electric displacement applied by the capacitance meter is very low (1–3 V), the Maxwell stress of the DE sensor induced by the third term of Eq. (7) could be neglected [12]. Then, the Cauchy stresses of the DE sensor reduce to the same form as Eq. (4). Similarly, the incompressible condition of the DE sensor leads to the following geometric equation,

$$r^3 - r_\mathrm{o}^3 = R^3 - R_\mathrm{o}^3, \quad R_\mathrm{o} \le R \le R_\mathrm{s}. \tag{8}$$

For both the DE sensor and the aneurysm wall, the Cauchy stresses must satisfy

$$\frac{\partial\sigma_{rr}}{\partial r} + 2\frac{\sigma_{rr} - \sigma_{\theta\theta}}{r} = 0, \tag{9}$$

from which we can get the expressions of the Cauchy stresses in the aneurysm wall and the DE sensor as follows,

$$\begin{aligned}\sigma_{rr}^{(\mathrm{A})} = \mu_\mathrm{A}&\left\{\left(\frac{4\eta\lambda_{\mathrm{e}\theta}^3 + 1}{6\lambda_{\mathrm{e}\theta}^4} - \frac{4\eta\lambda_{\mathrm{e}\theta,\mathrm{i}}^3 + 1}{6\lambda_{\mathrm{e}\theta,\mathrm{i}}^4}\right) - \frac{2}{3}\left(\eta^{4/3} - \eta^{-2/3}\right)\right.\\ &\times\left[\ln\frac{\left(\eta^{1/3}\lambda_{\mathrm{e}\theta,\mathrm{i}} - 1\right)\sqrt{\left(2\eta^{1/3}\lambda_{\mathrm{e}\theta} + 1\right)^2 + 3}}{\left(\eta^{1/3}\lambda_{\mathrm{e}\theta} - 1\right)\sqrt{\left(2\eta^{1/3}\lambda_{\mathrm{e}\theta,\mathrm{i}} + 1\right)^2 + 3}}\right.\\ &\left.\left.+\sqrt{3}\left(\arctan\frac{\sqrt{3}}{2\eta^{1/3}\lambda_{\mathrm{e}\theta} + 1} - \arctan\frac{\sqrt{3}}{2\eta^{1/3}\lambda_{\mathrm{e}\theta,\mathrm{i}} + 1}\right)\right]\right\}\\ &+ p_{\mathrm{blood}},\end{aligned} \tag{10a}$$

$$\sigma_{rr}^{(\mathrm{D})} = \frac{\mu_\mathrm{D}}{2}\left[\lambda_\theta^{-4} - \lambda_{\theta,\mathrm{s}}^{-4} + 4\left(\lambda_\theta^{-1} - \lambda_{\theta,\mathrm{s}}^{-1}\right)\right], \tag{10b}$$

where the boundary condition at the inner surface of the aneurysm wall subjected to the blood pressure p_blood, i.e., $\sigma_{rr}^{(\mathrm{A})}\Big|_{R=R_\mathrm{i}} = p_\mathrm{blood}$, and the traction free condition at the outer surface of the DE sensor, $\sigma_{rr}^{(\mathrm{D})}\Big|_{R=R_\mathrm{s}} = 0$ have been incorporated. In addition, the spherically isotropic growth condition ($g_\theta = g_\varphi$) is also considered. Here, the parameter $\eta = g_\theta/g_r$ represents the morphological size of the aneurysm in the thickness and circumferential directions, and, if assuming a constant ratio of growth velocity k in θ to r direction, the relationship between the growth in two diagonal directions can be written as $g_r = \frac{g_\theta+k-1}{k}$.

The Cauchy stresses in Eq. (10) must satisfy the continuity condition $\sigma_{rr}^{(A)}\Big|_{R=R_o} = \sigma_{rr}^{(D)}\Big|_{R=R_o}$ at the aneurysm/sensor interface, i.e.,

$$\mu_A\left\{\left(\frac{4\eta\lambda_{e\theta,o}^3+1}{6\lambda_{e\theta,o}^4}-\frac{4\eta\lambda_{e\theta,i}^3+1}{6\lambda_{e\theta,i}^4}\right)-\frac{2}{3}\left(\eta^{4/3}-\eta^{-2/3}\right)\right.$$
$$\times\left.\left[\ln\frac{\left(\eta^{1/3}\lambda_{e\theta,i}-1\right)\sqrt{\left(2\eta^{1/3}\lambda_{e\theta,o}+1\right)^2+3}}{\left(\eta^{1/3}\lambda_{e\theta,o}-1\right)\sqrt{\left(2\eta^{1/3}\lambda_{e\theta,i}+1\right)^2+3}}+\sqrt{3}\left(\arctan\frac{\sqrt{3}}{2\eta^{1/3}\lambda_{e\theta,o}+1}-\arctan\frac{\sqrt{3}}{2\eta^{1/3}\lambda_{e\theta,i}+1}\right)\right]\right\}$$
$$+p_{\text{blood}} = \frac{\mu_D}{2}\left[\lambda_{\theta,o}^{-4}-\lambda_{\theta,s}^{-4}+4\left(\lambda_{\theta,o}^{-1}-\lambda_{\theta,s}^{-1}\right)\right]. \tag{11}$$

At this stage, the geometrical parameters r_i, r_o, and r_s in the current configuration can be determined by solving the simultaneous equations including Eqs. (6), (8), and (11).

As for the spherical DE capacitor sensor, the electric field and the distribution of charges Q are regarded as uniform along the r direction. Then, the electric flux by using Gauss's law [17] is given by

$$\phi_{\text{net}} = \oint_{A_G} E_r \mathrm{d}A = E_r 4\pi r_G^2 = \frac{Q}{\varepsilon_0\varepsilon_r}, \tag{12}$$

where A_G is the Gaussian integral surface while ε_r is the relative permittivity of the DE sensor. The capacitance of the DE sensor is then obtained as

$$C = \frac{Q}{V} = \frac{Q}{\int_{r_o}^{r_s} E_r \mathrm{d}r_G} = \frac{4\pi\varepsilon_0\varepsilon_r r_s r_o}{r_s - r_o}, \tag{13}$$

where $V = \int_{r_o}^{r_s} E_r \mathrm{d}r_G$ is the potential difference between the two surfaces of the sensor, and the relative permittivity ε_r of ideal DE is taken as constant [16].

Taking an early-stage saccular aneurysm as the initial state, the radii are $R_i = 2$ mm and $R_o = 2.2$ mm, while the shear stress is $\mu_A = 0.6$ MPa [9]. For an aneurysm blood pressure $p_{\text{blood}} = 8.7$ kPa [3] and growth velocity ratio $k = 1.15$, the aneurysm wall ($\mu_D = 0$) bears tensile stress which increases monotonically with the natural growth while the inner surface always attains a maximum at any growth state (Fig. 2). This indicates that any possible rupture of the aneurysm should probably attribute to a high circumferential stress level at the inner surface. Meanwhile, the thickness of the aneurysm wall increases almost linearly with growth (Fig. 3), which is consistent with the statistical data of six patients' saccular aneurysms samples by Steiger et al. [9]. In addition, according to the suggested critical rupture stress 0.5 MPa [9], the critical size of the saccular aneurysm is about 10 mm (Fig. 3), also coincident with many other clinical statistics [3,4,6].

To monitor the growth and evaluate the stress level of the aneurysm, a thin layer of DE capacitance sensor (thickness 0.5 mm, $\mu_D = 0.01$ MPa) is mounted at the outer surface of the aneurysm. The correlation between the aneurysm state (circumferential stress and current outer diameter) and the relative capacitance C/C_0 is calculated, where C_0 is the initial capacitance value of

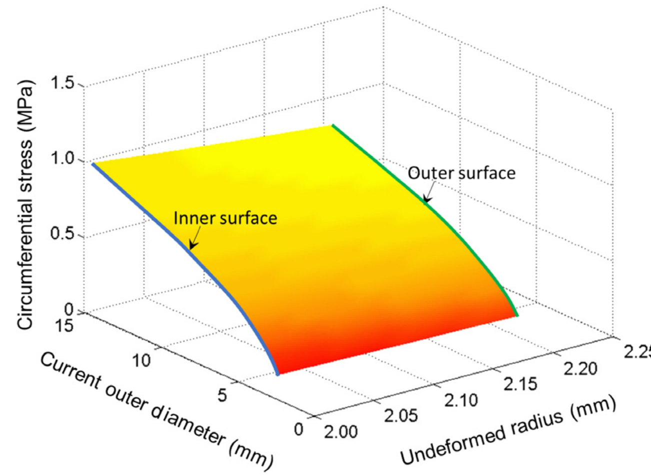

Fig. 2. Evolution of the transmural distribution of circumferential stress in the saccular aneurysm wall with the aneurysm growth ($\mu_D = 0$).

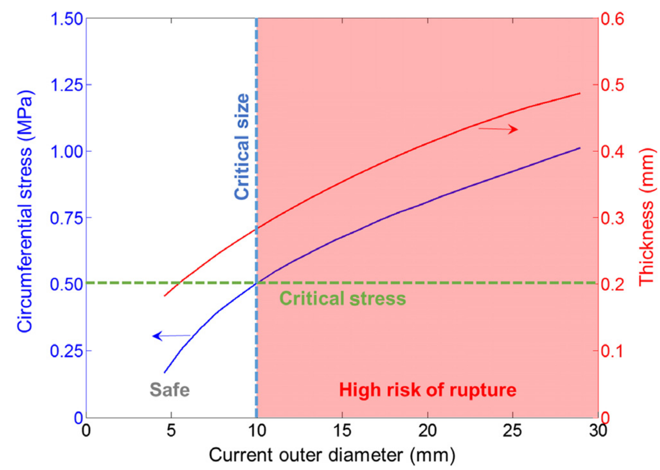

Fig. 3. Circumferential stress at the inner surface and wall thickness of the aneurysm during natural growth ($\mu_D = 0$).

the DE sensor. With the constraint effect of DE sensor on the aneurysm, the maximal outer diameter (critical size) prolongs to 12 mm if following the rule of critical stress (~0.5 MPa) for rupture (Fig. 4). This indicates that the DE sensor is not only able to gain the real-time growth information but also capable of postponing the aneurysm rupture. From the monitoring point, a relative capacitance of $C/C_0 \approx 30$ implies a high risk of rupture (Fig. 4).

We also calculated the sensitivity $\Delta\left(C/C_0\right)/\Delta\left(\sigma_{\theta\theta,i}^{(A)}/\mu_A\right)$ and resolution $\Delta\left(\sigma_{\theta\theta,i}^{(A)}/\mu_A\right)/\Delta\left(C/C_0\right)$ of the DE sensor for monitoring wall stress of the aneurysm during growing (Fig. 5). The sensitivity curve ascends while the resolution curve descends as the aneurysm enlarges, indicating that the DE sensor becomes more sensitive to the aneurysm growth and the accuracy for monitoring also increases. Especially in the high-risk stage ($C/C_0 > 30$), the resolution of the sensor is almost 0.1% of the critical stress 0.5 MPa, which suggests that the current DE sensor may achieve a prediction with an accuracy of about 0.5 kPa.

In conclusion, the current theoretical modeling can well simulate the natural growth of saccular aneurysms as compared to clinical statistics. The monitoring strategy proposed here is capable of providing multiple indicators including the size and wall stress to evaluate the rupture risk of saccular aneurysms. Results may serve as a useful reference for guiding in vivo experiments, and

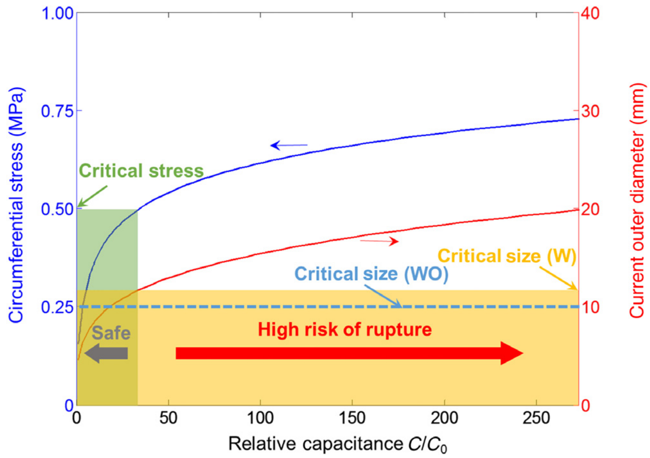

Fig. 4. Correlations between the relative capacitance and the growth state of the aneurysm (circumferential stress and the current outer diameter), where "W" for with and "WO" for without constraint effect of the DE sensor.

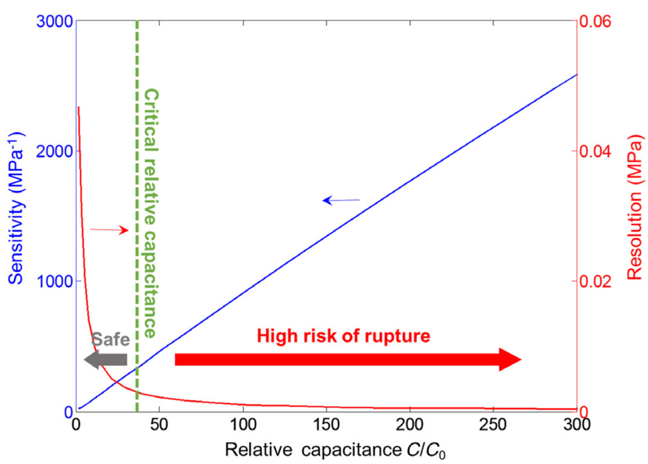

Fig. 5. Sensitivity and resolution of the DE capacitance sensor for monitoring the aneurysm growth.

the current method may also be extended to the monitoring of aneurysms with other shapes except that different deformation tensors should be used in the theoretical model. In addition, the correlation between the DE sensor and the growth state of saccular aneurysms determined by the current model may provide accurate real-time signals for patients and doctors, which is a supplement to traditional clinic diagnosis methods for forecasting the rupture of saccular aneurysms.

Acknowledgments

This work was supported by the National Natural Science Foundation of China (11322216, 11621062, and 11321202) and the Zhejiang Provincial Natural Science Foundation (LR13A020001).

References

[1] S.M. De la Monte, G.W. Moore, M.A. Monk, et al., Risk factors for the development and rupture of intracranial berry aneurysms, Am. J. Med. 78 (1985) 957–964.
[2] G.G. Ferguson, Intracranial arterial aneurysms—a surgical perspective, in: Handbook of Clinical Neurology, Shirley Decker-lucke, 1989, pp. 41–87.
[3] J.D. Humphrey, P.B. Canham, Structure, mechanical properties, and mechanics of intracranial saccular aneurysms, J. Elast. Phys. Sci. Solids 61 (2000) 49–81.
[4] D.O. Wiebers, Unruptured intracranial aneurysms — risk of rupture and risks of surgical intervention, N. Engl. J. Med. 339 (1998) 1725–1733.
[5] D.O. Wiebers, Unruptured intracranial aneurysms: Natural history, clinical outcome, and risks of surgical and endovascular treatment, Lancet 362 (2003) 103–110.
[6] S. Asari, T. Ohmoto, Growth and rupture of unruptured cerebral aneurysms based on the intraoperative appearance, Acta Med. Okayama 48 (1994) 257–262.
[7] M. Shojima, M. Oshima, K. Takagi, et al., Magnitude and role of wall shear stress on cerebral aneurysm: Computational fluid dynamic study of 20 middle cerebral artery aneurysms, Stroke 36 (2004) 1933–1938.
[8] S. Scott, G.G. Ferguson, M.R. Roach, Comparison of the elastic properties of Human intracranial arteries and aneurysms, Can. J. Physiol. Pharm. 50 (1972) 328–332.
[9] H.J. Steiger, R. Aaslid, S. Keller, et al., Strength, elasticity and viscoelastic properties of cerebral aneurysms, Heart Vessels 5 (1989) 41–46.
[10] J.D. Humphrey, Continuum biomechanics of soft biological tissues, Proc. R. Soc. A: Math. Phys. Eng. Sci. 459 (2003) 3–46.
[11] B. Li, Y.P. Cao, X.Q. Feng, et al., Surface wrinkling of mucosa induced by volumetric growth: Theory, simulation and experiment, J. Mech. Phys. Solids 59 (2011) 758–774.
[12] C.F. Lü, Y.K. Du, Theoretical modeling for monitoring the growth of fusiform abdominal aortic aneurysms using dielectric elastomer capacitive sensors, Int. J. Appl. Mech. 8 (2016) 1640010.
[13] E.K. Rodriguez, A. Hoger, A.D. Mcculloch, Stress-dependent finite growth in soft elastic tissues, J. Biomech. 27 (1994) 455–467.
[14] Y. Wang, C. Zhang, W. Chen, An analytical model to predict material gradient and anisotropy in bamboo, Acta Mech. 226 (2015) 1–15.
[15] H.J. Steiger, Pathophysiology of development and rupture of cerebral aneurysms, Acta Neurochir. Suppl. 48 (1990) 1–57.
[16] A. Dorfmann, R.W. Ogden, Nonlinear electroelastostatics: Incremental equations and stability, Internat. J. Engrg. Sci. 48 (2010) 1–14.
[17] N.C. Goulbourne, S. Son, J.W. Fox, Self-sensing McKibben actuators using dielectric elastomer sensors, Proc. Soc. Photo-Opt. Instrum. Eng. 6524 (2007) 652414.